

Dynamic Modeling and Control of a Fuel Cell Hybrid Vehicle with Onboard Fuel Processor

Lucas Nieto Degliuomini, Diego Feroldi,
David Zumoffen, and Marta Basualdo

*CIFASIS-CONICET. Bv 27 de Febrero 210 bis. Rosario, Santa Fe
S2000EZP Argentina
(nieto,feroldi,zumoffen,basualdo@cifasis-conicet.gov.ar)*

Abstract: The transient behavior of a Fuel Processor System to produce Hydrogen from bio-ethanol with high performance, coupled with a Proton Exchange Membrane Fuel Cell is modeled. The Ethanol Processor is based on a previous steady state design, optimized to work with maximum efficiency around 10 kW of rated power. From the dynamic rigorous model, a linearized model is identified to apply a systematic procedure to synthesize the control structure. The Fuel Cell System is then hybridized with supercapacitors as auxiliary power source, to lower the overall consumption of hydrogen, hence of bio-ethanol too. The entire vehicle is tested using standard driving cycles, widely utilized in related literature and to measure pollutant emissions. The overall behavior reaches the expectations and is capable of fulfilling the requirements of urban and highway scenarios, and also suggests the possibility of resizing the components to improve fuel economy.

Keywords: Hybrid vehicles, Energy management strategies, Bio-ethanol fuel processor, Fuel cells, Plant-wide control structures

1. INTRODUCTION

Fuel cells are devices that convert chemical energy (often in the form of hydrogen) into electricity, without passing through a combustion stage. Fuel Cell Hybrid Vehicles (FCHV) is a promising application that has taken more and more importance in the last years and is considered the most attractive long-term option for passenger cars. Hybridization in FCHV consists in adding a supplementary energy storage element (e.g., a battery or a superCapacitor (UC) bank) to the primary power source, i.e. Proton Exchange Membrane Fuel Cell (PEMFC), in order to adequate optimally the energy generation to the consumption with almost zero emission. This procedure has important advantages, allowing a greater reduction of the hydrogen consumption, and its economical importance has been recently remarked in Offer et al. (2010).

In order to properly manage and distribute the power requirements between the auxiliary power sources, an energy management strategy must be applied. Some works have appeared regarding to the power management of hybrid vehicles with multiple energy sources, such as fuel cell, battery and supercapacitor [Thounthong et al. (2009) and Li et al. (2009)]. The management strategy used in this work is presented in detail in Feroldi et al. (2009).

In Biset et al. (2009) has been presented a preliminary plant-wide control structure for the process of hydrogen production from bio-ethanol to be used in a PEMFC, accounting only steady-state information. In this work, the operational conditions for the PEMFC were adopted from recommendations given by Pukrushpan et al. (2004). In this last work, a deep study about control of fuel cell systems, with focus on air-flow control was presented. Hence, believing on the high quality of that work, in this paper is used the same control oriented model of the PEMFC which is considered as a benchmark. In Pukrushpan et al. (2004), several control strategies are proposed accounting abrupt current demand from the vehicle. They concluded that the air supply must be promptly increased to replenish the cathode with oxygen.

There are few publications regarding fuel processors dynamic behavior, some using methanol as raw material, such as Chuang et al. (2008), and very recently some publications on using ethanol to produce hydrogen. Some of these are Aicher et al. (2009) and García et al. (2009). Even though they present dynamic models, or experimental results, and use them to synthesize control structures, they do not contemplate the energy integration, and the combination of the Fuel Cell System with energy storage devices, which makes this technology economically feasible and highly interacted. Previously mentioned research works highlighted main difficulties and objectives to account in the operation of fuel processors and cell systems, which are vital to assure catalysts working life, and to avoid components mechanical or thermal damage, because they are very sensitive. This is the first work that deals

* The authors want to acknowledge the financial support from CONICET (Consejo Nacional de Investigaciones Científicas y Técnicas) and ANPCYT (Agencia Nacional de Promoción Científica y Técnica) from Argentina.

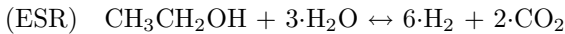
with the entire hybrid vehicle integrated, meaning Fuel Processor Plant, Fuel Cell System, Energy Storage System, Energy Management Strategy and Powertrain models. It is rigorously tested using standardized driving cycles.

2. THE MODEL

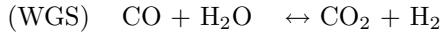
2.1 Fuel Processor System

The Fuel Processor System (FPS) (illustrated in Fig. 4) consists of a Bio-Ethanol Steam Reforming (ESR) plug flow reactor, where most of the conversion of ethanol to H_2 is made. Carbon monoxide (CO) which poisons the fuel cell catalyst is produced in the ESR, so additional processing is needed to remove this substance. There are three reactors that configure the cleaning system; these are two Water Gas Shift (WGS), one of high temperature (fast) and the other of low temperature, that favors the equilibrium of the reaction to higher conversion rates of CO. The third is a Preferential Oxidation of Carbon monoxide (CO-PrOx) reactor, where oxidation of CO into CO_2 is made; also, the undesired oxidation of H_2 occurs, so the catalyst is selected to improve the conversion of CO.

Ethanol and vaporized water are mixed and then supplied to the ESR reactor, to produce ethanol decomposition:



The overall reaction is endothermic, and heat requirement is supplied by a burner, which is fed with ethanol and compressed air. The transfer of heat is achieved passing the hot gases through the jacket of the reformer. The produced reaction inside the WGS is:



This reaction produces heat and creates more hydrogen. Levels of CO are still high even after the two WGS reactors, so the final elimination is made in the CO-PrOx reactor, which produces the oxidation of CO. The WGS reaction takes place in this reactor too. Oxygen is injected into the CO-PrOx, the amount needed is about twice the stoichiometric relation to have a good selectivity and satisfy the requirements of the FC.

The plug flow reactors are modeled as 20 lined-up Continuous Stirred Tank Reactors (CSTR). The molar flow between two volumes is given by the orifice flow equation as a function of upstream pressure, and downstream pressure. Further details on the dynamic modeling, process constraints and normal behavior can be seen in Nieto Degliuomini et al. (2009).

2.2 Proton Exchange Membrane Fuel Cell

Fuel cells convert chemical energy directly into electrical energy. They are constituted by an anode, where the H_2 is injected, and a cathode, where the oxidant, normally air is injected. The electrodes are separated by a membrane that allows the proton exchange and contribute to the oxidation reaction to produce electrical power. The cell generates an open-circuit voltage which is affected by a number of losses (activation, concentration and ohmic) that leads to a useful actual voltage. Pukrushpan et al. (2004) presents a rigorous dynamic model of a PEMFC

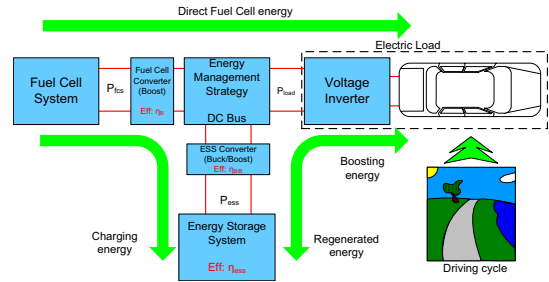


Fig. 1. Configuration of the entire vehicle

which is used in this work. It is possible to be adapted to produce a maximum power of 10 kilowatts. Transient behavior of manifold filling, membrane hydration, the air compressor and the heat management are included in the model. Interaction between processes are also included.

2.3 Computational Model Implementation

The pressure requirements are satisfied with compressors and turbines modeled in HYSYS. In addition, it supports the important data bank information for the different components. In addition, the LNG tool in HYSYS, that solves material and heat balances for multi-stream exchangers and heat exchangers networks. On the other hand, the dynamic model of the reactors is developed in MATLAB, which integrates the differential equations. The communication interface is performed by the use of the spreadsheets in HYSYS and a specific library for doing the corresponding data transference and updating at scheduled sampling time between both programs.

Heat Integration The heat integration in the model is performed by the LNG tool working in a pseudo dynamic mode. It is called by MATLAB for determining the instantaneous temperature values of the different cold and hot streams of the process. Therefore, it is assumed that the dynamic effect of the heat exchangers network is neglected. The minimum heat requirement of the system and the minimum heat to be evacuated can be computed for each operating point or with the system under different disturbances.

Hybridization In order to integrate the Fuel Processor and Fuel Cell System with an entire vehicle and the energy management strategy, the detailed model developed in ADVISOR is used (Markel et al. (2002)). The FCS and the strategy originally presented are replaced by the ones discussed in section 4. The integrated power train along with the energy flows is shown in Fig. 1.

3. CONTROL STRUCTURE DESIGN

The main objectives of the FPS control are to maintain H_2 levels on the anode of the FC and keeping the temperatures of the reactors set and FC prevent damages, maintaining the system efficiency. A correct H_2 level prevents starvation which can cause permanent damage, and overfeeding will lead to Hydrogen waste. In addition, the CO levels of the anode inlet stream must be low. A brief description of the systematic control structure design given in Zumoffen and Basualdo (2009) is applied.

Table 1. Manipulated variables

u_1	Water to ESR inlet
u_2	Exchanged heat Q
u_3	Ethanol to Burner
u_4	Oxygen to Burner
u_5	Oxygen to CO-PrOx
u_6	CM voltage

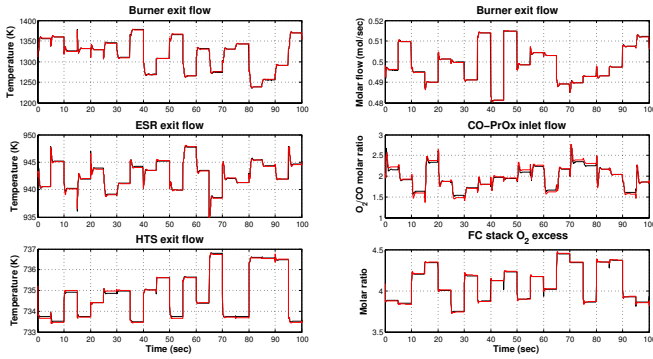


Fig. 2. Validation results obtained through the identified linear model. Simulation variables in black and linearized in red.

3.1 Linearization of the dynamic model

The first step for defining the control structure design is to obtain a linearized model. In order to do this, a simulation must be done applying step random uniform changes in all the manipulated variables available (shown in table 1) and in the considered disturbances (current demand I_{st} and fresh ethanol molar fraction). Therefore, all the recorded data is processed for obtaining a linearized model through a specific identification method.

The classical algorithm named n4sid method developed by Van Overschee and De Moor (1994) and implemented in Matlab by Ljung (2002) is used here. This technique allows to determine an estimate of the system matrices ($\hat{\mathbf{A}}$, $\hat{\mathbf{B}}$ and $\hat{\mathbf{C}}$) and model order using singular value decomposition from the impulse response Hankel matrix. It is obtained from the data by solving a linear least squares problem.

The validation results, obtained from the linearized model confronted to those given by the simulation of the rigorous one, are shown in Fig. 2. A state-space representation with 49 states was developed, adjusting separately the FC output variables and the variables that pertain to the FPS. The order of both models was chosen according to the minimal mean square error for the stationary state. A very good approximation (either for stationary states and transients) is achieved with the reduced order model.

3.2 Selection of controlled variables

The selection of controlled variables is based on Internal Model Control (IMC) theory for non-square process, steady-state deviations and stochastic integer optimization (combinatorial problem). The search is oriented to achieve the less interactive square system (\mathbf{G}_s) within the control structure shown at Fig. 3. The measurement selection is performed so as to minimize the sum of square deviation

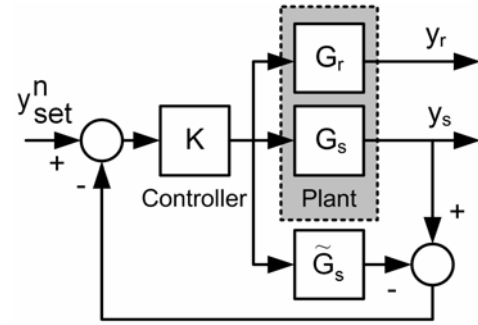


Fig. 3. Square IMC control structure for non-square plant (SSD) of those uncontrolled variables while the square system is under perfect control. The controller block K in Fig. 3 is implemented as a full IMC controller.

Therefore, the idea is to choose a proper \mathbf{G}_s able to minimize the SSD. For the process under consideration the potential number of measurements is $m = 16$ (flows, temperatures, molar ratios and concentrations) and the number of manipulated variables is $n = 6$ (detailed in table 1). Thus, the combinatorial problem dimension is $m!/(n!(m-n)!) = 8008$. Usually, to lower the dimensionality of the problem, process experience and engineering judgement needs to be applied. In order to obtain an approach without involving any heuristics, data mining algorithms are suggested to solve the minimization problem. Particularly, in this work, the search is performed by genetic algorithm (GA) strategy based on integer optimization tools to find the best solution in terms of minimum SSD. The chosen variables to be controlled are ESR temperature, Burner temperature, HTS temperature, CO-PrOx temperature, Burner exit molar flow and Oxygen ratio.

3.3 Pairing variables for control design

The optimal sensor network in a square system was defined. In this stage, the pairing of the variables for deciding the final plant-wide control structure is detailed. In this case, the GA solution using the SSD index represents the lower interacting structure (by SSD definition). Thus, a Relative Gain Array (RGA) analysis is carried out for the optimal solution.

The resulting optimal RGA is shown in Table 2, and the synthesized control structure in Fig. 4. Basically, the control of the ESR exit temperature is achieved manipulating the exchanged heat with combustion gases. The HTS exit temperature is controlled with the inlet flow of water to the processor. The exit temperature of the CO-PrOx is regulated with its air flow inlet. The temperature of the gases leaving the burner is manipulated with the amount of ethanol feed. The exit flow of the burner is controlled by the entering air. The O_2 excess ratio in the stack is controlled with the entering oxygen. The prior loop of H_2 productivity is regulated with the inlet of fresh feed of ethanol.

The next step is testing the proposed control structure under the required scenarios for this plant. The controllers tuning is carried out by using the dynamic linear model identified previously following the recommendations given in Rivera (2007) and Rivera et al. (1986).

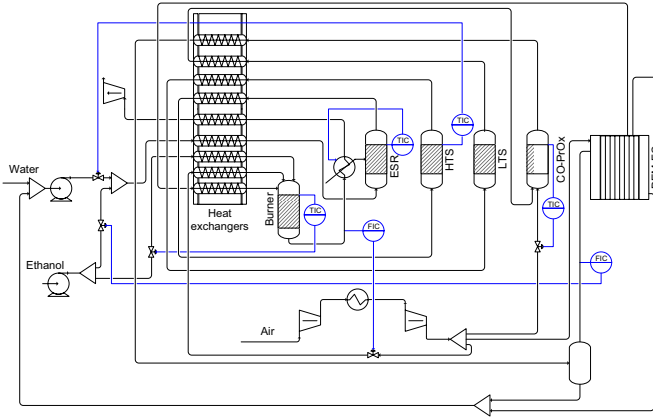


Fig. 4. Implemented control structure

Table 2. The best obtained RGA (steady-state)

	u_1	u_2	u_3	u_4	u_5	u_6
Y_4	0.989	-0.036	-0.002	0.042	0.006	0.001
Y_1	-0.020	1.049	0.017	-0.042	-0.003	-0.001
Y_3	0.001	-0.002	0.908	0.104	-0.010	0.000
Y_{12}	0.001	0.007	0.095	0.898	0.000	0.000
Y_6	0.029	-0.017	-0.017	-0.002	1.004	0.003
Y_{14}	-0.000	-0.001	0.000	-0.000	0.004	0.997

4. ENERGY MANAGEMENT STRATEGY

The management strategy used in this work, is given in detail in Feroldi (2009). It is based on the Fuel Cell System (FCS) efficiency map and it operates the FCS preferably in its point of maximum efficiency in order to improve the hydrogen economy, although the final operating point of the FCS is determined based on the actual power demand and the state of energy (SoE) of the Energy Storage System (ESS). The FCS power command is determined according to the following rules (nomenclature is explained in table 3). If the load power is

$$P_{fcs,lo}\eta_B \leq P_{load}(k) \leq P_{fcs,hi}\eta_B \quad (1)$$

and, the SoE is

$$SoE_{lo} \leq SoE(k) \leq SoE_{hi} \quad (2)$$

where $P_{fcs,hi}$ is

$$P_{fcs,hi} = P_{fcs,max}\eta_B X_{fcs,hi} \quad (3)$$

and $X_{fcs,hi}$ is a fraction of the maximum FCS power; then, the FCS is operated in its point of maximum efficiency

$$P_{fcs}(k) = P_{fcs,maxeff} \quad (4)$$

The remaining power to achieve the load demand flows from or to the ESS according to

$$P_{ess}(k) = \min \left\{ \frac{(P_{load}(k) - P_{fcs}(k)\eta_B)}{\eta_{B/B}\eta_{ess}}, (SoE(k) - SoE_{min})k_{ess} \right\} \quad (5)$$

if $P_{load}(k) > P_{fcs,maxeff}$ (discharging mode), or

$$P_{ess}(k) = -\min \left\{ \frac{P_{load}(k) - P_{fcs}(k)\eta_B}{\eta_{ess}\eta_{B/B}}, (SoE(k) - SoE_{max})k_{ess} \right\} \quad (6)$$

if $P_{load}(k) < P_{fcs,maxeff}$ (charging mode).

If the load power is

$$P_{fcs,hi}\eta_B \leq P_{load}(k) \leq P_{fcs,max}\eta_B \quad (7)$$

Table 3. nomenclature utilized

Symbol	Description	Value
k	Current time	Seconds
$P_{fcs,lo}$	Lower net power	4000 W
$P_{fcs,hi}$	Higher net power	8000 W
P_{load}	Demanded Power	W
P_{fcs}	FC net power	W
P_{ess}	ESS output power	W
$P_{fcs,max}$	Maximum net power	10000 W
$P_{fcs,maxeff}$	Maximum efficiency net power	8000 W
η_B	FC converter efficiency	0.95
$\eta_{B/B}$	ESS converter efficiency	0.95
η_{ess}	ESS efficiency	0.95
SoE_{lo}	Lower SoE	0.4
SoE_{hi}	Higher SoE	0.8
SoE_{min}	Minimum SoE	0.3
SoE_{max}	Maximum SoE	0.9
T_{off}	Time to turn off FC	60 sec

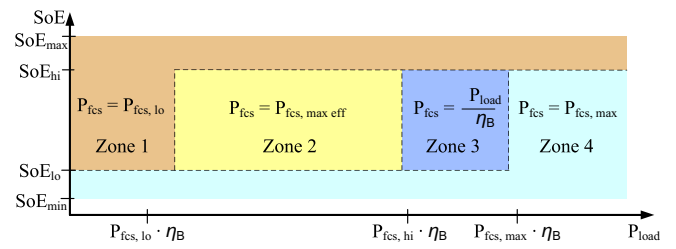


Fig. 5. FCS operating point for the strategy based on efficiency map

and, the SoE is

$$SoE_{lo} \leq SoE(k) \leq SoE_{hi} \quad (8)$$

then, the FCS is operated in load following mode

$$P_{fcs}(k) = \frac{P_{load}(k)}{\eta_B} \quad (9)$$

and $P_{ess}(k)$ is as indicated in (6) or (5).

On the other hand, if

$$P_{load}(k) \geq P_{fcs,max}\eta_B \text{ and } SoE(k) \leq SoE_{hi} \quad (10)$$

or

$$SoE(k) \leq SoE_{lo} \quad (11)$$

then, the FCS is operated at its maximum power

$$P_{fcs}(k) = P_{fcs,max} \quad (12)$$

and $P_{ess}(k)$ is as indicated in (5). If, on the contrary

$$P_{load}(k) \leq P_{fcs,lo}\eta_B \text{ and } SoE(k) \geq SoE_{lo} \quad (13)$$

or

$$SoE(k) \geq SoE_{hi} \quad (14)$$

then, the FCS is working at its lower operating point

$$P_{fcs}(k) = P_{fcs,lo} \quad (15)$$

and $P_{ess}(k)$ is as in (6). Additionally, if $P_{load}(k) = 0 \forall t \in [k1, k2]$ with $(k2 - k1) > T_{off}$, and, $SoE(k) > SoE_{hi}$ with $k > k2$, then, the FCS is turned off to avoid unnecessary hydrogen consumption because the parasitic losses in the FCS. Fig. 5 indicates the FCS operating point as a function of the $SoE(k)$ and the load power $P_{load}(k)$. The transition between operating points is performed according to the constraints concerning the maximum fall power rate and the maximum power rate.

5. DISTURBANCES TO THE HYBRID VEHICLE

In order to evaluate the performance of a given hybrid vehicle, standard driving cycles are widely utilized in the literature. They represent urban and highway scenarios and were originally stated for measuring pollutant emissions and fuel economy of engines (DieselNet. Emission test cycles. Online, 2005). In Figs. 6 and 7 the speed demands corresponding to: the Highway Fuel Economy Cycle (HWFET), the New European Driving Cycle (NEDC), the Urban Dynamometer Driving Schedule (UDDS) and the Federal Test Procedure (FTP) are plotted. As can be seen, high power requirements take place during a relatively short fraction of time. If there is no energy storage, the FCS must meet the highest peak power and, therefore, the efficiency of a FCS is strongly degraded at low powers. Thus, if no hybridization is present, the FCS has to work in large periods of time at a low efficiency zone. On the contrary, with an additional power source and a suitable energy management strategy it is possible to avoid these unfavorable operating zones. In a fuel cell hybrid system it is possible to boost the FCS supplying energy to the load from the energy storage system. This energy was previously charged from the FCS or regenerated from the load, e.g., from regenerative braking in automotive applications.

6. APPLICATION RESULTS

Simulations of the Hybrid Vehicle for the driving cycles are done, and the results shown in Figs. 6 and 7. For each group of figures, the speed requirements; power split between the FC and storage system; O_2 excess ratio in the cathode; working zone, and H_2 production are plotted. It can be seen that both the management strategy and the FCS are capable of working properly against the wide range of power demands proposed by the driving cycles. For the FTP, between 1430 and 2000 seconds, the FCS is turned off, because the power demanded by the bus is null and the SoE of the UC is greater than 0.9. For sustained high power demands, such as HWFET, the SoE tends to decrease, against the tendency for the other driving cycles, which is to rise.

In Fig. 8 the ethanol consumption for the different driving cycles are presented, it is remarkable that for the pure fuel cell case, the needed power output could not be achieved, because the FC net power is less than the required in all cases. On the other hand, in all driving cycles, hybridization represents ethanol economy, consuming less than the pure FC case. In fact, in some of them, the hybrid vehicle consumption is very close to the ideal case, which is the case when the FC is always operating in maximum efficiency.

7. CONCLUSIONS

From the simulated results it is concluded that the proposed FCHV, that includes the entire power train, from the raw material, bio-ethanol, up to the drive train of the vehicle, gives a quite good performance tested with urban and highway scenarios. Two main reasons justify the successful results: the proper control structure and the energy management strategy. The first one is provided

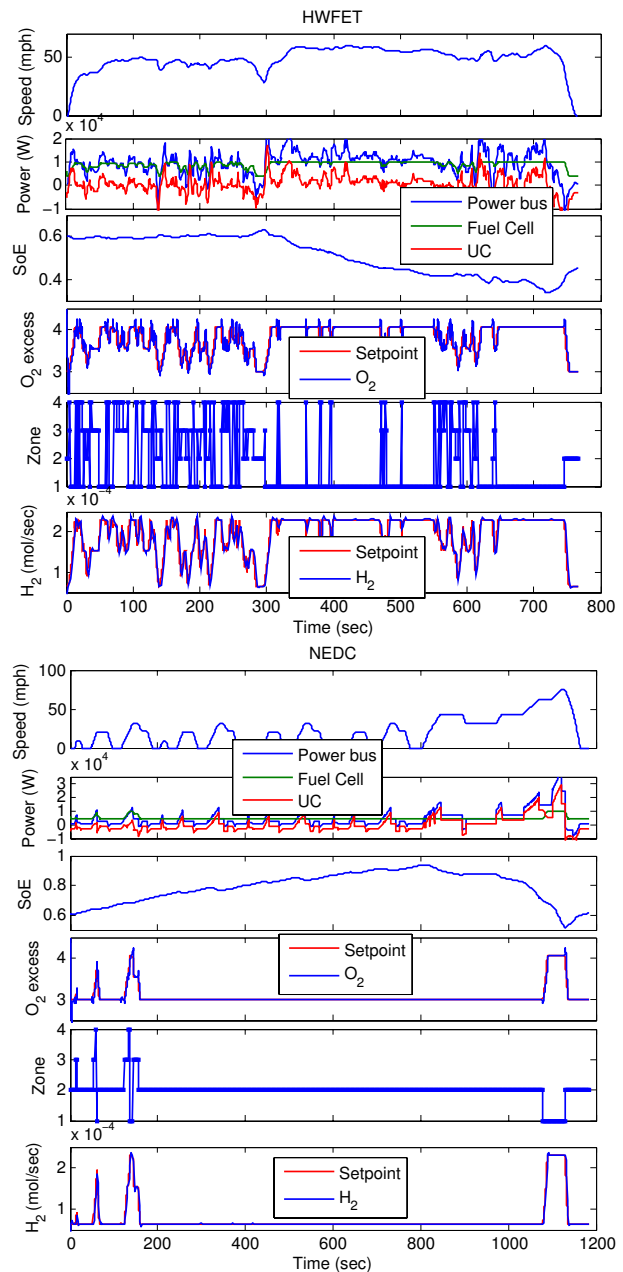


Fig. 6. Simulation results for HWFET and NEDC

via a systematic procedure able for keeping the plant under the desired conditions. The second one, is capable of the system gives the required power, working inside the good efficiency zones. In addition, for all driving cycles, hybridization consumes less bio-ethanol than the FC working alone. The SoE presents a tendency to fall or raise during the cycles, producing the FC variable working zone, with the consequent efficiency drop. So, it is suggested the implementation of a FC with a wider zone of high efficiencies, to avoid the operation at lower performance.

REFERENCES

- Aicher, T., Full, J., and Schaadt, A. (2009). A portable fuel processor for hydrogen production from ethanol in a 250w fuel cell system. *International journal of hydrogen energy*, 34, 8006–8015.

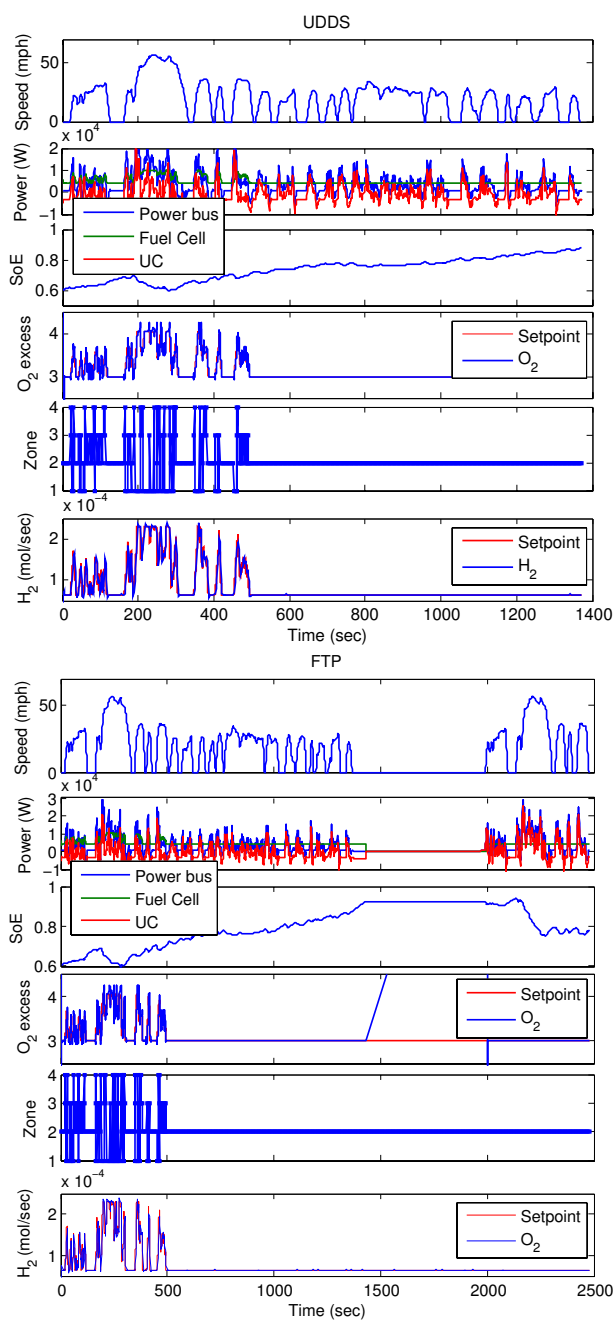


Fig. 7. Simulation results for UDDS and FTP

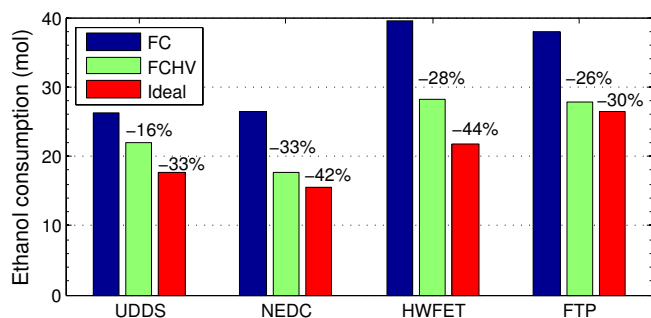


Fig. 8. Bio-ethanol consumption for the driving cycles

Biset, S., Nieto Degliuomini, L., Basualdo, M., Garcia, V.M., and Serra, M. (2009). Analysis of the control structures for an integrated ethanol processor for proton exchange membrane fuel cell systems. *Journal of Power Sources*, 192(1), 107–113.

Chuang, C.C., Chen, Y.H., Ward, J.D., Yu, C.C., Liu, Y.C., and Lee, C.H. (2008). Optimal design of an experimental methanol fuel reformer. *International journal of hydrogen energy*, 33, 7062–7073.

Feroldi, D. (2009). *Control and design of PEM fuel cell-based systems*. Ph.D. thesis, Universitat Politècnica de Catalunya.

Feroldi, D., Serra, M., and Riera, J. (2009). Energy management strategies based on efficiency map for fuel cell hybrid vehicles. *Journal of Power Sources*, 190(2), 387–401.

García, V.M., López, E., Serra, M., Llorca, J., and Riera, J. (2009). Dynamic modeling and controllability analysis of an ethanol reformer for fuel cell application. *International journal of hydrogen energy*. doi: 10.1016/j.ijhydene.2009.09.064.

Li, X., Xu, L., Hua, J., Lin, X., Li, J., and Ouyang, M. (2009). Power management strategy for vehicular-applied hybrid fuel cell/battery power system. *Journal of Power Sources*, 191(2), 542–549.

Ljung, L. (2002). System identification toolbox. for use with matlab. The Mathworks.

Markel, T., Brooker, A., Hendricks, T., Johnson, V., Kelly, K., Kramer, B., O’Keefe, M., Sprik, S., and Wipke, K. (2002). Advisor: a system analysis tool for advanced vehicle modeling. *Journal of Power Sources*, 110, 255–266.

Nieto Degliuomini, L., Biset, S., Domnguez, J., and M.S., B. (2009). Control oriented dynamic rigorous model of a fuel processor system and fuel cell stack. *Computer Aided Chemical Engineering*, 27, 609–614.

Offer, G.J., Howey, D., Contestabile, M., Clague, R., and Brandon, N.P. (2010). Comparative analysis of battery electric, hydrogen fuel cell and hybrid vehicles in a future sustainable road transport system. *Energy Policy*, 38(1), 24–29.

Pukrushpan, J.T., Stefanopoulou, A.G., and Peng, H. (2004). *Control of Fuel Cell Power Systems: Principles, Modeling, Analysis and Feedback Design*. Springer.

Rivera, D.E. (2007). Una metodología para la identificación integrada con el diseño de controladores IMC-PID. *Revista Iberoamericana de Automática e Informática Industrial*, 4(4), 129–134.

Rivera, D.E., Morari, M., and Skogestad, S. (1986). Internal model control 4. pid controller design. *Ind. Eng. Chem. Proc. Des. and Dev.*, 25, 252.

Thounthong, P., Rael, S., and Davat, B. (2009). Energy management of fuel cell/battery/supercapacitor hybrid power source for vehicle applications. *Journal of Power Sources*, 193(1), 376–385.

Van Overschee, P. and De Moor, B. (1994). N4sid: Subspace algorithms for the identification of combined deterministic-stochastic systems. *Automatica*, 30(1), 75–93.

Zumoffen, D. and Basualdo, M. (2009). Optimal sensor location for chemical process accounting the best control configuration. *Computer Aided Chemical Engineering*, 27, 1593–1598.